JNTM JOURNAL of NEW TECHNOLOGY and MATERIALS

*Journal of New Technology and Materials*

**Vol. 15, No. 1 (2025), 36–45**

RESEARCH ARTICLE

# Impedance-Normalized Operating-Window Selection of Trimetallic Cu-Co-Mo Heterostructures for Low-Voltage Alkaline Water Electrolysis

Jiacheng Fang[1], Ray H. Baughman[2,*] and Song-Zhi Liu[1]

[1]Department of Material Functions and design, Nagoya Institute of technology, Gokiso-Cho Showa-ku, Nagoya, Aichi, 466-8555 Japan. [2]NanoTech Institute, University of Texas at Dallas, 800 West Campbell road, Richardson, TX75080, 75080 USA

*Correspondence: ray.baughman@utdallas.edu

Received date: August 13, 2024; Accepted date: December 18, 2024

## Abstract

Successful operation of an alkaline water electrolyzer involves more than simply employing the best half-cell for each reaction separately, as an efficient electrode requires the combination of active reaction sites, effective charge transfer, acceptable price and low potential difference between the two electrodes. In order to improve the descriptor-based selection criteria for trimetallic Cu-Co-Mo heterostructures, this work takes into account CuCoMo-LDH, CuCoMo-P and CuCoMo-S electrodes as complete systems, not individual oxygen evolution and hydrogen evolution catalysts. The calculation is made based on experimental values of surface area, impedance, overpotential, potential difference, Faradaic efficiency and electrode price in order to create the impedance-normalized operating window method. CuCoMo-P demonstrates the highest performance, possessing the greatest BET surface area ($21.35\,m^2\,g^{-1}$), the largest ECSA ($440\,cm^2$), the smallest charge-transfer resistance during HER ($1.61\,\Omega$), the smallest potential difference during electrolysis at $10\,mA\,cm^{-2}$ (1.393 V) and the lowest energy intensity per 1000 L of produced hydrogen, approximately equal to 3.33 kW h. CuCoMo-LDH is still the best catalyst for OER reaction at the $50\,mA\,cm^{-2}$ current density, however, the difference in OER overpotentials is much lower than the difference in HER overpotentials and the difference in the potential difference.

*Keywords: alkaline water electrolysis, CuCoMo phosphide, trimetallic heterostructure, bifunctional electrocatalyst, charge-transfer resistance, operating-window selection, hydrogen production*

## 1 Introduction

Electrochemical hydrogen generation by water splitting faces significant materials challenges in the context of renewable power-to-fuel conversion since this process can be achieved efficiently only when the electrolyzer works with small voltage losses, robust electrodes and reasonable cost per material. Thermodynamically speaking, it is necessary to apply voltage greater than 1.23 V to split water, while an actual alkaline cell requires extra potential due to the kinetic and thermodynamic complexities associated with the kinetics of water oxidation reaction (OER), hydrogen evolution reaction (HER), interfacial polarization, ionic and gas transfer [1, 2].

In addition, evaluating the half-cell properties and performance of electrocatalysts presents an issue, since the descriptor emphasized in an article often fails to reveal which material is the best for a full-cell water splitting application. Overpotential for OER, overpotential for HER, Tafel slope, ECSA, BET surface area and voltage in two-electrode system are important and informative measures, but none of them takes into account the whole electrode, e.g., sluggish HER can be compensated by a very low OER overpotential, poor BET surface area by ineffective ion adsorption, or great Tafel slope by the inability to catalyze OER. Therefore, standardized comparison is important not only for reporting precision but also for avoiding choosing inappropriate electrode for an alkaline cell [3, 4].

Layered double hydroxides (LDH) offer an advantageous starting point for studying alkaline OER since these lamellar compounds can host transition metal sites that can develop active oxyhydroxide-like phase upon oxidation. Co- and Fe-based hydroxides are good examples of the way in which metal site properties, redox behavior and coordination environment can improve oxygen intermediates production. At the same time, some problems with the use of hydroxide electrodes include low electrical conductivity and subpar HER. Thus, even though a hydroxide catalyst performs well in an anodic half cell, it can result in increased cell voltage once applied to both cathodic and anodic parts of an alkaline electrolyzer [5–7].

In the context of HER, transition metal phosphides represent another class of promising materials. Bonding of metal atoms with sulfur creates conditions for polarizing electrode surface, improving electron conductivity and tuning hydrogen binding energies, which made phosphides good candidates for investigating HER. In an alkaline medium, this approach is particularly relevant since proton supply in this medium depends greatly on water dissociation and hydroxide availability. Besides, phosphides can undergo electrodeposition, creating a conductive inner core while reconstructing anodic surface, and thus providing an electrode with an ability to catalyze reactions in both water splitting branches. In other words, phosphide-based electrodes are interesting subjects of operating window analysis [8–10].

Like phosphides, transition metal sulfides represent yet another group of electrodes of interest for analyzing water splitting processes. Molybdenum sulfide and analogous chalcogenides were shown to benefit from rich defects at the surface and edges of the crystal as the factors facilitating hydrogen generation. However, in case of the sulfide-based electrodes, insufficient electrical conductivity or limited accessible area of sulfide surface can lower the overall performance despite a large nominal composition. Therefore, judging such an electrode solely by its composition is inappropriate, and its performance should be estimated on the basis of the relations between morphological and kinetic properties [11–13].

For studying the effect of structure and composition on water splitting performance, the electrodes with similar composition but dissimilar architecture are a good choice. The heterostructure of cobalt, copper and molybdenum can help in achieving good results due to the differences between these metals. Thus, Co allows to catalyze the production of hydroxide/oxyhydroxide, Mo modifies binding properties of electrons and hydrogen intermediates, and Cu influences water adsorption at the active surface sites and reorganization of the charge distribution. The difference between LDH, phosphide and sulfide structures based on Cu-Co-Mo is particularly interesting since this set allows making comparative conclusions about the efficiency of each structure [14–16].

As far as HER and OER studies show, nowadays a proper selection of catalyst relies greatly on relating its catalytic performance with engineering criteria such as charge transfer resistance, ECSA and cell voltage. Since the electrolyzer consists of cathode and anode, it is unproductive to choose its components on the basis of a single electrode property (e.g., isolated OER overpotential). For instance, in some cases it is preferable to select an electrode with slightly worse isolated performance, but higher HER kinetics, smaller resistance and two-electrode cell voltage. The importance of this consideration is the key idea of the current work because CuCoMo-LDH, CuCoMo-P and CuCoMo-S do not rank identically in terms of either isolated or full-cell criteria.

Therefore, the main objective of this paper is the development of impedance-normalized operating-window approach for comparing CuCoMo-LDH, CuCoMo-P and CuCoMo-S materials. The descriptors of the approach include BET surface area, ECSA, HER charge transfer resistance, OER overpotential, HER overpotential, voltage in two-electrode system, calculated voltage-derived energy intensity and cost per area. Although there are other important techniques for materials assessment (e.g., Raman or XPS spectroscopy), here, too, the scope of the problem is quite particular: to find out which Cu-Co-Mo heterostructure can produce the strongest operating window taking into account all surface, kinetic and voltage-related parameters.

## 2 Energy, Surface, Cost, and Impedance Metrics

### 2.1 Numerical descriptor basis and electrode set

The numerical descriptor set consists of the tabulated CuCoMo-LDH, CuCoMo-P and CuCoMo-S electrocatalytic values and will be used for the impedance-normalized operating window calculation [16]. These values correspond to BET specific surface area, ECSA, OER and HER overpotentials, HER charge-transfer resistance, two-electrode cell voltage, Faradaic efficiency, hydrogen generation rate and estimated production cost. The present study employs those descriptors to answer the following selection question: which Cu-Co-Mo derivative provides a better balance of full-cell performance when considering active surface population, interfacial impedance, voltage demand and areal material cost?

CuCoMo-LDH, CuCoMo-P and CuCoMo-S may be considered as structurally similar but functionally distinct Cu-Co-Mo heterostructures deposited on nickel foam. CuCoMo-LDH represents the layered hydroxide precursor, CuCoMo-P corresponds to the phosphide-based electrode and CuCoMo-S is the sulfided version of the catalyst. This comparison is helpful because the metal set is identical but the surface morphology, charge-transport pathway and electrochemical anion structure are different for the derivatives. For that reason, the observed differences in performance can be rationalized in terms of the conversion effect on catalytic interfacial properties.

It can be seen in the morphology sequence of Figure 1 that CuCoMo-LDH is a relatively compact layer, whereas the

phosphidized catalyst exhibits a porous network of interconnected sites. The sulfided CuCoMo has a densely packed particulate morphology. This observation is crucial since it determines the possibility of electrolyte access to active sites and electronic transfer from the substrate without excessive polarization.

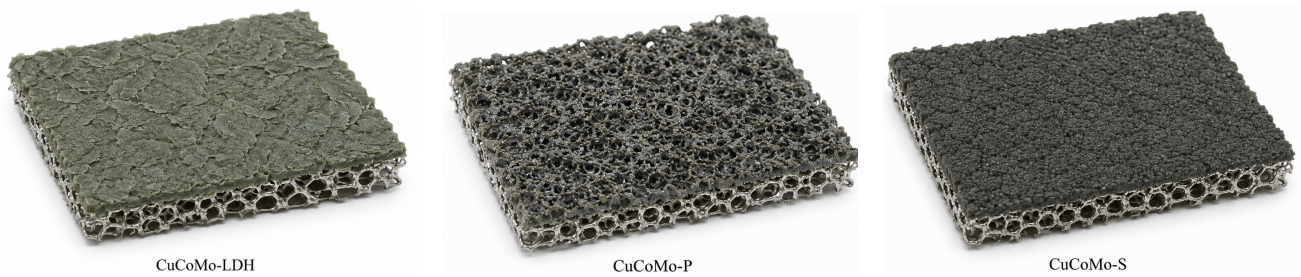


**(a)** CuCoMo-LDH **(b)** CuCoMo-P **(c)** CuCoMo-S

**Figure 1.** Morphology of the Cu-Co-Mo heterostructures on nickel foam.

It would be too early to conclude that an open surface is beneficial. In order to generate electrochemically active area and low charge-transfer resistance, it must produce measurable electrochemical activity. That is why the distinction established visually is carried into the numerical descriptor sequence and cannot be regarded as evidence of the superior catalytic function in isolation.

**Table 1.** Numerical descriptors for impedance-normalized materials selection.

| Electrode | Cost ($/cm$^2$) | BET SSA ($m^2$/g) | ECSA ($cm^2$) | $\eta_{OER,50}$ (mV) | $\eta_{HER,50}$ (mV) | $R_{ct,HER}$ (Ω) | $V_{10}$ (V) |
|---|---|---|---|---|---|---|---|
| CuCoMo-LDH | 0.051 | 7.436 | 162.5 | 307 | 215 | 10.04 | 1.427 |
| CuCoMo-P | 0.053 | 21.350 | 440.0 | 331 | 117 | 1.61 | 1.393 |
| CuCoMo-S | 0.052 | 2.261 | 80.0 | 311 | 265 | 47.66 | 1.540 |
| $RuO_2$ ‖ Pt/C reference | – | – | – | 369[a] | 83[b] | – | 1.554 |

[a]OER overpotential of $RuO_2$ reference catalyst at 50 mA $cm^{-2}$. [b]Pt/C HER overpotential at −50 mA $cm^{-2}$. $V_{10}$ denotes the two-electrode voltage at 10 mA $cm^{-2}$; for CuCoMo-S, the measured low-current full-cell value is retained for the noble-metal comparison.

The descriptors in Table 1 demonstrate the need for the developed approach quite explicitly. CuCoMo-LDH features the best OER overpotential at 50 mA $cm^{-2}$. However, CuCoMo-P boasts the highest BET surface area, ECSA, smallest HER overpotential and HER charge-transfer resistance. Thus, the choice of an optimal electrode requires the combined evaluation of the voltage and the other parameters.

## 2.2 Impedance-normalized operating-window method

The first of the proposed descriptors translates the two-electrode cell voltage into an energy value per liter of $H_2$:

$$\mathcal{E}_{1000} = \frac{2FV_{\text{cell}}}{3.6 \times 10^6} \left(\frac{1000}{V_m}\right), \tag{1}$$

where $\mathcal{E}_{1000}$ is measured in kWh/(1000 L $H_2$), $F$ is the Faraday constant, $V_{\text{cell}}$ is two-electrode voltage and $V_m$ is the molar gas volume in L/mol. Equation 1 is introduced as a common voltage reference to facilitate comparisons, and not as an energy-production model. All processes outside the direct water-splitting reaction, such as compressor work, drying of product gases, thermal management etc., are omitted. The purpose is to assess the performance of the electrodes under equal assumptions regarding the operation conditions and process chain.

The meaning of Equation 1 is that the millivolt difference between voltages can be translated into $H_2$ production costs. A lower $V_{\text{cell}}$ directly results in a lower energy requirement for producing 1000 L of $H_2$. This is a crucial advantage for comparing CuCoMo-LDH and CuCoMo-P since their voltage values differ by only tens of millivolts.

The second descriptor is based on interfacial impedance and electrochemically active surface area:

$$\mathcal{K}_{\text{HER}} = \frac{A_{\text{ECSA}}}{R_{\text{ct,HER}}}, \tag{2}$$

where $A_{\text{ECSA}}$ is the electrochemically active area in $cm^2$ and $R_{\text{ct,HER}}$ is the HER charge-transfer resistance in Ω. High

$\mathcal{K}_{\mathrm{HER}}$ implies that the catalyst possesses a large population of active sites with excellent charge-transport properties. While this descriptor is not a universal constant of kinetics, it does evaluate the quality of electroactive surfaces by rewarding efficient charge-transport pathways and punishing high charge-transfer resistances.

Equation 2 becomes extremely meaningful in the context of symmetrical electrolyzers where the cathode branch can become a bottleneck for voltage optimization. This particular descriptor is introduced to find out whether the electrochemically active surface created by the conversion processes is efficiently coupled with the HER-relevant charge transport mechanism.

The third of the described descriptors combines the information on surface development and areal cost:

$$\mathcal{S}_c = \frac{S_{\mathrm{BET}}}{C_A}, \tag{3}$$

where $S_{\mathrm{BET}}$ is the BET specific surface area in $\mathrm{m}^2/\mathrm{cm}^2$ and $C_A$ is the areal material cost in $\$/\mathrm{cm}^2$. Equation 3 is an indicator of surface yield that measures the surface area produced by a catalyst per unit of areal cost.

The interpretative power of Equation 3 becomes clear from the consideration of the CuCoMo materials. As it can be seen, their estimated costs are almost identical. This means that a relatively high $\mathcal{S}_c$ is achieved due to increased surface area and not due to cost reduction. Hence, the surface yield value indicates whether a structural conversion leads to an increase in physical surface area.

Finally, the voltage-saving value relative to the noble-metal reference system is introduced:

$$\mathcal{V}_s = \frac{V_{\mathrm{ref},10} - V_{10}}{C_A}, \tag{4}$$

where $V_{\mathrm{ref},10}$ is the reference two-electrode cell voltage at $10\,\mathrm{mA\,cm^{-2}}$. Equation 4 evaluates the low-current voltage performance of non-noble electrodes by dividing the savings by areal cost. Since all three CuCoMo materials have very similar $C_A$, their separation will depend primarily on voltage performance.

The meaning of Equation 4 is practical. A relatively cheap material that does not improve or worsen performance compared to a noble electrode is not particularly desirable for industrial use. Therefore, this descriptor differentiates between the inexpensive catalysts and efficient electrodes.

## 3 Electrocatalytic Performance and Operating-Window Analysis

### 3.1 Surface architecture and active-area utilization

The surface-area descriptors show that phosphidation produces the most accessible Cu-Co-Mo architecture in the evaluated set. CuCoMo-P has a BET surface area of $21.35\,\mathrm{m^2\,g^{-1}}$, compared with $7.436\,\mathrm{m^2\,g^{-1}}$ for CuCoMo-LDH and $2.261\,\mathrm{m^2\,g^{-1}}$ for CuCoMo-S. This means that the phosphide has nearly three times the physical surface area of the hydroxide and more than nine times that of the sulfide. Such a difference is significant because BET area reflects micro- and mesostructural surface development, even though not every measured surface atom necessarily participates in electrochemical turnover.

The ECSA values confirm that the surface enrichment of CuCoMo-P is also electrochemically relevant. CuCoMo-P reaches $440\,\mathrm{cm}^2$, while CuCoMo-LDH and CuCoMo-S reach $162.5\,\mathrm{cm}^2$ and $80\,\mathrm{cm}^2$, respectively. The phosphide electrode therefore provides not only a larger physical surface but also a greater population of sites accessible to the electrolyte within the potential window used for capacitance-derived surface estimation. This distinction is essential because a rough material can still perform poorly when domains are blocked, poorly wetted or electronically isolated.

The coupled ECSA-impedance map in Figure 2 places the surface and transport descriptors on the same visual scale. CuCoMo-P occupies the desirable region of high accessible area and low HER resistance, while the sulfide sample is shifted toward low ECSA and high resistance. The bubble-size representation adds a third dimension by showing that the BET advantage of the phosphide is not disconnected from its electrochemical response.

The map in Figure 2 explains why morphology alone is not enough. CuCoMo-P is selected because the open surface generates both high ECSA and low resistance; CuCoMo-S, by contrast, shows that structural conversion can produce a coating that is present on nickel foam but not optimally connected for cathodic charge transfer. The figure therefore supports the central argument that the useful electrode is the one in which surface population and interfacial kinetics are aligned.

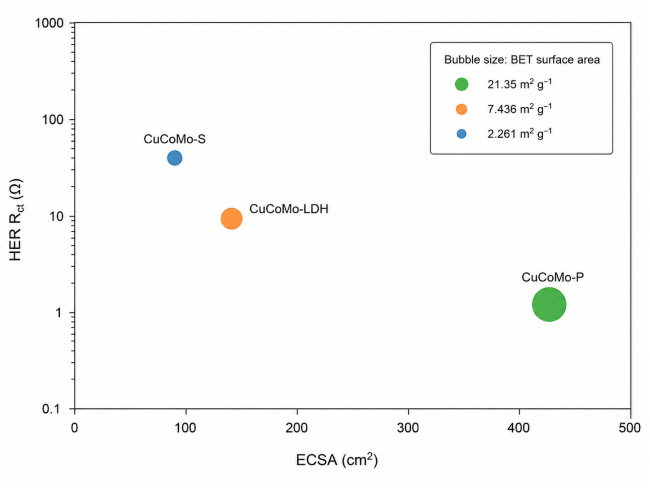


**Figure 2.** Coupled surface-accessibility and impedance map. ECSA is plotted against HER charge-transfer resistance, and the bubble size represents BET surface area. The phosphide electrode combines the largest accessible area with the smallest HER interfacial resistance, explaining why its morphological advantage is transferred into electrochemical performance.

**Table 2.** Descriptors calculated from the operating values using the impedance-normalized method.

| Electrode | $\mathcal{K}_{\mathrm{HER}}$ ($\mathrm{cm}^2\ \Omega^{-1}$) | $\mathcal{S}_c$ (SSA/cost) | $\Delta V_{10}$ (mV) | $\mathcal{V}_s$ (V/\$ $\mathrm{cm}^{-2}$) | $\mathcal{E}_{1000}$ (kWh/1000 L) | $1.23/V_{10}$ (%) |
|---|---|---|---|---|---|---|
| CuCoMo-LDH | 16.19 | 145.8 | 127 | 2.49 | 3.41 | 86.2 |
| CuCoMo-P | 273.29 | 402.8 | 161 | 3.04 | 3.33 | 88.3 |
| CuCoMo-S | 1.68 | 43.5 | 14 | 0.27 | 3.68 | 79.9 |
| $RuO_2 \parallel Pt/C$ | – | – | 0 | – | 3.72 | 79.2 |

The derived descriptor table gives the first complete numerical answer to the selection problem. CuCoMo-P reaches $\mathcal{S}_c = 402.8$, compared with 145.8 for CuCoMo-LDH and 43.5 for CuCoMo-S, indicating that the phosphide route produces the largest physical surface reservoir per unit areal cost. Since the three Cu-Co-Mo electrodes differ by only about \$0.002 $\mathrm{cm}^{-2}$ in estimated cost, this separation is controlled by surface generation rather than by a large price difference.

The same table shows a much larger separation in $\mathcal{K}_{\mathrm{HER}}$. CuCoMo-P reaches 273.29 $\mathrm{cm}^2\ \Omega^{-1}$, whereas CuCoMo-LDH reaches 16.19 $\mathrm{cm}^2\ \Omega^{-1}$ and CuCoMo-S reaches only 1.68 $\mathrm{cm}^2\ \Omega^{-1}$. This means that the phosphide descriptor is approximately 16.9 times higher than the LDH value and more than 160 times higher than the sulfide value. Such a difference is too large to be a minor secondary effect; it identifies cathodic accessibility and charge transfer as the decisive reasons why the full-cell ranking favors CuCoMo-P.

## 3.2 Half-cell activity and bifunctional balance

The OER values alone favor CuCoMo-LDH by a narrow margin. CuCoMo-LDH reaches 50 $\mathrm{mA\,cm}^{-2}$ at 307 mV, while CuCoMo-S and CuCoMo-P require 311 mV and 331 mV, respectively. A conventional OER-only interpretation would therefore select the hydroxide. That outcome is reasonable because hydroxide-derived surfaces can form redox-active metal oxyhydroxide motifs that are well suited to oxygen-intermediate formation under alkaline anodic conditions.

The HER branch changes the materials decision. CuCoMo-P requires only 117 mV at $-50$ $\mathrm{mA\,cm}^{-2}$, compared with 215 mV for CuCoMo-LDH and 265 mV for CuCoMo-S. The phosphide therefore reduces the cathodic overpotential by 98 mV relative to the hydroxide and by 148 mV relative to the sulfide at the same current density. This gain is larger than the OER penalty of CuCoMo-P relative to CuCoMo-LDH, so the overall selection changes when both gas-evolution reactions are considered.

The bifunctional trade-off is made explicit in Figure 3. The left branch confirms the narrow anodic advantage of CuCoMo-LDH, while the right branch shows the much stronger cathodic advantage of CuCoMo-P. This comparison is important because a symmetric cell cannot isolate the better OER electrode from its weaker HER behavior; the same material must carry both kinetic burdens.

The overpotential comparison in Figure 3 also clarifies why the noble-metal reference does not determine the CuCoMo ranking. Pt/C remains highly active for HER, but the full-cell reference voltage is higher than that of CuCoMo-P at the selected current density. The practical message is that a bifunctional non-noble material can be favored when its total cell behavior, accessible area and interfacial resistance are considered together rather than when individual noble-metal half-cell values are treated separately.

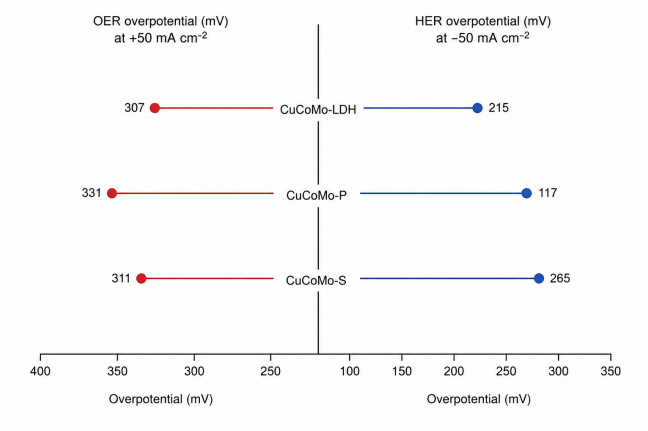


**Figure 3.** Bifunctional overpotential balance at 50 mA cm$^{-2}$. The left branch compares OER overpotentials at positive current density and the right branch compares HER overpotentials at negative current density. CuCoMo-P sacrifices only a modest amount of OER activity relative to CuCoMo-LDH while producing the strongest HER response among the Cu-Co-Mo electrodes.

The control-electrode trends support a cooperative trimetallic effect. Monometallic and bimetallic hydroxide comparators show weaker activity than the Cu-Co-Mo electrodes, indicating that the combined metal environment contributes to improved catalytic response. In mechanistic terms, Cu may assist water adsorption and local charge redistribution, Co may provide redox-active hydroxide/oxyhydroxide sites, and Mo may tune electronic states and hydrogen-intermediate binding. The performance trend therefore reflects composition and structural conversion acting together rather than a simple support effect.

## 3.3 Charge-transfer resistance and the phosphide advantage

Electrochemical impedance provides the strongest physical rationale for the phosphide ranking. The HER charge-transfer resistance of CuCoMo-P is 1.61 Ω, far lower than 10.04 Ω for CuCoMo-LDH and 47.66 Ω for CuCoMo-S. This order indicates that the phosphide interface requires much less additional driving force to move electrons into hydrogen-forming intermediates. Lower resistance also means that a larger share of the applied voltage can be used for reaction chemistry instead of being consumed by interfacial polarization.

The large $\mathcal{K}_{\mathrm{HER}}$ value for CuCoMo-P arises from the convergence of high ECSA and small $R_{\mathrm{ct}}$. CuCoMo-LDH has a moderate ECSA but a larger resistance, so its effective kinetic-accessibility number is limited. CuCoMo-S has both the smallest ECSA and the highest resistance, producing the weakest descriptor. CuCoMo-P is therefore not merely a material with a low HER overpotential; it is an electrode architecture in which accessible surface and electronic transport reinforce each other.

This point is important for practical electrode design. As current density increases, isolated active sites are insufficient unless they remain electronically connected to the substrate and ionically accessible to the electrolyte. The phosphide architecture likely provides a more continuous conductive path from nickel foam to Cu-Co-Mo catalytic domains while maintaining a porous surface. Such an arrangement distributes current over a larger number of participating sites, reduces local kinetic stress and helps explain why the phosphide maintains the lowest two-electrode voltage at both low and higher current density.

## 3.4 Full-cell voltage, energy intensity and voltage efficiency

The two-electrode values confirm the ranking predicted by the impedance-normalized descriptors. CuCoMo-P requires only 1.393 V at 10 mA cm$^{-2}$, compared with 1.427 V for CuCoMo-LDH, 1.540 V for CuCoMo-S and 1.554 V for the $RuO_2 \,\|\, Pt/C$ reference. The voltage saving of CuCoMo-P relative to the reference is 161 mV. It is also 34 mV lower than CuCoMo-LDH and 147 mV lower than CuCoMo-S. These differences are meaningful because electrolyzer energy consumption scales directly with operating voltage.

At 50 mA cm$^{-2}$, CuCoMo-P continues to show the lowest full-cell voltage among the three Cu-Co-Mo electrodes, requiring 1.633 V. CuCoMo-LDH and CuCoMo-S require 1.732 V and 1.818 V, respectively. The current-dependent comparison in Figure 4 confirms that the phosphide curve remains below the LDH and sulfide curves across the measured current window. This result is important because it shows that the phosphide advantage is not restricted to the low-current reference point used for many electrocatalyst comparisons.

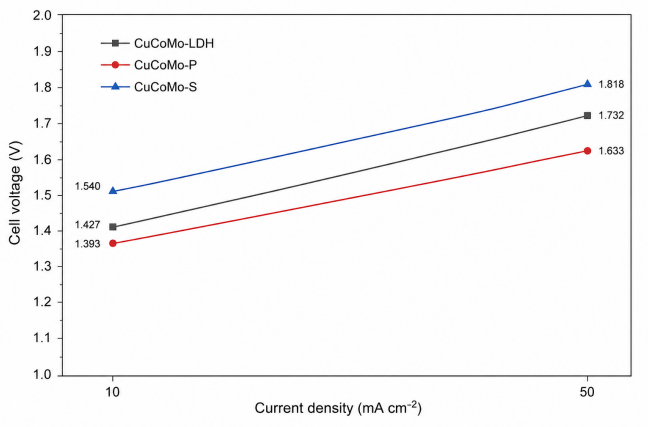


**Figure 4.** Two-electrode cell voltage as a function of current density for CuCoMo-LDH, CuCoMo-P and CuCoMo-S. CuCoMo-P maintains the lowest full-cell voltage at both 10 mA cm$^{-2}$ and 50 mA cm$^{-2}$, indicating that its impedance and active-area advantages remain important as operating current increases.

The current-sweep plot in Figure 4 strengthens the selection argument by showing persistence rather than a single-point advantage. If CuCoMo-P were favored only at 10 mA cm$^{-2}$, the ranking might be sensitive to the chosen comparison current. Instead, its lower voltage at 50 mA cm$^{-2}$ indicates that the conductivity and active-area benefits remain relevant when stronger gas-evolution flux is required.

Using Equation 1, the voltage at 10 mA cm$^{-2}$ corresponds to an approximate electrical energy demand of 3.33 kW h per 1000 L of $H_2$ for CuCoMo-P. The corresponding values are 3.41 kW h for CuCoMo-LDH, 3.68 kW h for CuCoMo-S and 3.72 kW h for the $RuO_2 \,||\, Pt/C$ reference. These are voltage-derived comparison values, not complete system-energy requirements. Their significance lies in the relative order: the phosphide electrode converts the same hydrogen-output basis into the smallest calculated electricity demand.

The paired voltage and energy-intensity comparison in Figure 5 shows how the measured voltage order is translated into the hydrogen-output scale. The electrode with the lowest $V_{10}$ also gives the lowest $\mathcal{E}_{1000}$ because the calculation is directly proportional to cell voltage. The figure therefore prevents the energy descriptor from appearing as an abstract formula and ties it to the experimentally meaningful voltage gap among the materials.

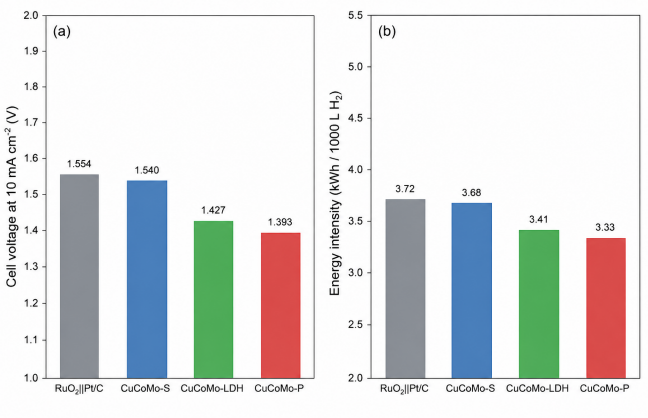


**Figure 5.** Voltage and energy-intensity comparison at the 10 mA cm$^{-2}$ reference condition. Panel (a) compares cell voltages for the noble-metal reference and the three Cu-Co-Mo electrodes, while panel (b) converts those voltages into approximate electricity demand per 1000 L of $H_2$. CuCoMo-P gives the lowest value in both panels.

The paired representation in Figure 5 confirms that the CuCoMo-P advantage is modest in absolute voltage but meaningful in direction and consistency. The difference between CuCoMo-P and CuCoMo-LDH is smaller than the difference between CuCoMo-P and CuCoMo-S, which means that the hydroxide remains a credible anodic material. However, the phosphide remains the preferred full-cell electrode because it lowers both the measured voltage and the calculated energy intensity under the same assumptions.

The apparent voltage-efficiency descriptor $1.23/V_{10}$ gives the same conclusion. CuCoMo-P reaches 88.3%, while CuCoMo-LDH reaches 86.2%, CuCoMo-S reaches 79.9% and the reference reaches 79.2%. The practical interpretation is that CuCoMo-P operates closest to the thermodynamic water-splitting voltage among the evaluated cells. Even a

difference of a few tens of millivolts can become significant during continuous operation, so the 161 mV reference-cell voltage saving is a meaningful materials-level advantage.

**Table 3.** Interpretive ranking of the Cu-Co-Mo electrodes across coupled selection criteria.

| Criterion | Preferred electrode | Key numerical basis |
|---|---|---|
| Lowest isolated OER overpotential | CuCoMo-LDH | 307 mV at 50 mA $cm^{-2}$ |
| Lowest isolated HER overpotential | CuCoMo-P | 117 mV at −50 mA $cm^{-2}$ |
| Highest accessible active area | CuCoMo-P | ECSA = 440 $cm^2$ |
| Lowest HER interfacial impedance | CuCoMo-P | $R_{ct}$ = 1.61 Ω |
| Lowest symmetric full-cell voltage | CuCoMo-P | $V_{10}$ = 1.393 V |
| Highest cost-normalized voltage saving | CuCoMo-P | $\mathcal{V}_s$ = 3.04 V/$ $cm^{-2}$ |

The table above summarizes the reasons why the final answer differs from the OER-only answer. CuCoMo-LDH is first for isolated anodic electrochemistry, but CuCoMo-P dominates the list of criteria most related to symmetric-cell performance: HER overpotential, accessible area, HER impedance, two-electrode voltage and cost-normalized voltage saving. CuCoMo-S is excluded not due to lack of activity; it is excluded due to HER resistance and low accessible surface area, which hinder the realization of OER electrochemistry in practice.

Figure 6 visualizes the same idea using the normalized operating window representation. High values correspond to advantageous features of each descriptor, and the most comprehensive advantage is reflected by the enclosed area. CuCoMo-P encloses the largest region due to its combined high ECSA, high BET surface area, low HER resistance, low HER overpotential and low cell voltage.

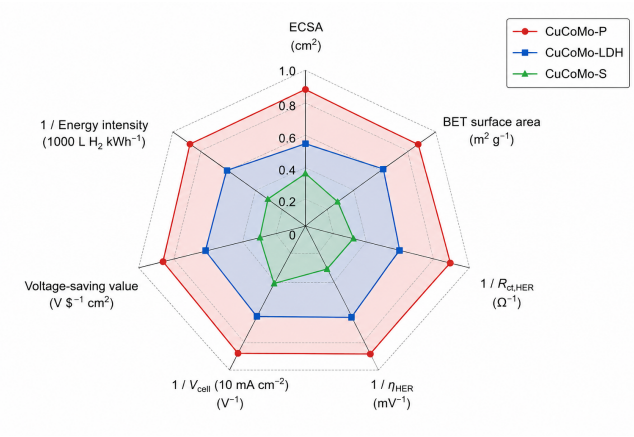


**Figure 6.** Normalized multi-descriptor operating window for CuCoMo-LDH, CuCoMo-P and CuCoMo-S. Higher values denote more favorable electrode behavior for each axis after normalization. The phosphide electrode encloses the largest area because its high ECSA, high BET surface area, low HER resistance, low HER overpotential and low cell voltage work together rather than as independent characteristics.

Figure 6 is beneficial due to the way it helps to avoid misinterpretations related to the selective choice of an optimal descriptor. CuCoMo-LDH scores well on the OER axis, but its weak HER-related properties limit the size of the operating window. CuCoMo-S scores worse across all criteria except for low HER resistance, but the absence of both open surface and strong cathodic charge transfer results in poor overall operating ability. CuCoMo-P is therefore chosen not due to the presence of a single desirable feature, but as a result of the combination of many of them.

## 3.5 Cost-normalized deployment value and Faradaic utilization

Similar areal material costs can be estimated for the three Cu-Co-Mo heterostructures: \$0.051 $cm^{-2}$ for CuCoMo-LDH, \$0.053 $cm^{-2}$ for CuCoMo-P and \$0.052 $cm^{-2}$ for CuCoMo-S. With the help of this knowledge, one can state that the performance superiority of CuCoMo-P is not achieved at the price of excessive material use. CuCoMo-P gives the largest value of voltage savings per dollar of material cost, $\mathcal{V}_s$, namely 3.04 V per dollar per square centimeter compared to 2.49 for CuCoMo-LDH and 0.27 for CuCoMo-S. As expected, CuCoMo-P reduces cell voltage most effectively per dollar invested in material cost.

The cost-normalized operating-window diagram in Figure 7 allows the comparison between areal cost and value of voltage saving relative to the noble metal. According to this figure, the phosphide material achieves the largest value of the latter and has the second-lowest former in the Cu-Co-Mo group. In other words, a higher areal cost of the reference noble metal does not translate into a higher voltage-savings value.

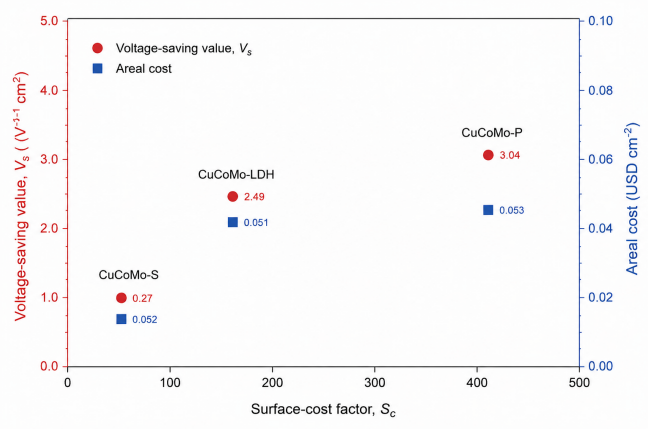


**Figure 7.** Cost-normalized voltage-saving comparison. The markers show the value of voltage savings relative to the noble-metal reference and the material cost. CuCoMo-P has the highest voltage-saving value without a substantial cost increase compared to the other Cu-Co-Mo materials.

The previous analysis demonstrates how useful the cost plot in Figure 7 is for deployment-oriented evaluation. The material cost does not allow the reader to think that the performance is improved due to the use of expensive materials. Instead, a slight difference in the cost value corresponds to a much larger difference in the cell-voltage reduction potential.

One more proof of the deployment-oriented value of the phosphide material comes from Faradaic efficiency. CuCoMo-P gives 98.7% Faradaic efficiency, generates hydrogen at the rate of 3.4 mL min$^{-1}$ and has the hydrogen-production cost of \$0.12255 per 1000 L. These values support the importance of the low voltage because the high Faradaic efficiency suggests that almost no charge is wasted on parasitic reactions, which might otherwise weaken the value of the reduced voltage.

### 3.6 Mechanistic implications

It becomes clear from the descriptor analysis above that certain mechanistic explanations may be offered. Conversion of Cu-Co-Mo hydroxide into phosphide is likely to increase surface openness and conductivity of Cu-Co-Mo-P along with the creation of the favorable cathodic environment. Polarization of metal sites and tuning of the hydrogen adsorption energy, which is nearly thermoneutral at −0.11 eV for CuCoMo-P, can occur as a result of phosphorus addition. At the same time, phosphides tend to exhibit higher conductivities, meaning that the additional expense paid for electron transfer is decreased.

On the contrary, the OER side of copper cobalt molybdate should be viewed with a focus on the dynamic surface transformation process rather than composition alone. Under anodic polarization, phosphides may evolve metal oxyhydroxide-like surface motifs involved in oxygen evolution. This mechanism does not mean that phosphidation is ineffective due to loss of electrical contact because the phosphide-rich conductive core is retained after the surface change. As demonstrated in the operating-window analysis, CuCoMo-P has the second-best OER overpotential, but the most advantageous HER properties and low symmetric-cell voltage.

Finally, the CuCoMo-LDH sample is discussed as an extreme case of an optimal half-cell material that fails in full-cell performance. The latter may occur due to the insufficient contribution of cathodic electrochemical activity and the resulting increased cell voltage. CuCoMo-S, on the other hand, cannot serve as the best example of a low-voltage bifunctional catalyst in spite of sulfide composition due to its low surface area, low ECSA and high HER resistance.

### 3.7 Direct answer to the research question

In accordance with the research question stated in the introduction, it must be answered what Cu-Co-Mo heterostructure exhibits the highest deployment-relevant operating window. CuCoMo-P is chosen here as the best Cu-Co-Mo material in terms of operating electrochemistry due to its advantageous values of several key parameters including HER overpotential, ECSA, impedance resistance and cell voltage. The reason for choosing this specific sample is explained above. CuCoMo-P gives the highest BET surface area, ECSA, HER overpotential and lowest cell voltage at 10 mA cm$^{-2}$. The resulting value of energy intensity based on the voltage-derived estimate equals 3.33 kW h per 1000 L $H_2$. This value is smaller than those of CuCoMo-LDH, CuCoMo-S and the noble-metal reference.

## 4 Conclusions

The research problem has been solved by proving the superior deployment value of CuCoMo-P, which is explained by its advantageous properties of surface area, impedance resistance and low two-electrode voltage. Though CuCoMo-LDH achieves the lowest OER overpotential at 50 mA cm$^{-2}$, the normalized impedance-related descriptors demonstrate the

following values for CuCoMo-P: $\mathcal{K}_{\mathrm{HER}} = 273.29\ \mathrm{cm}^2\ \Omega^{-1}$ and $\mathcal{S}_c = 402.8$. Furthermore, CuCoMo-P has the lowest cell voltage at $10\,\mathrm{mA\,cm}^{-2}$, namely 1.393 V. This leads to the value of energy intensity of 3.33 kW h per liter of hydrogen. This value is smaller than those calculated for CuCoMo-LDH, CuCoMo-S and the noble metal.

## References


[1] J. A. Turner, Sustainable hydrogen production, *Science*, 2004, 305, 972–974.

[2] K. Zeng and D. Zhang, Recent progress in alkaline water electrolysis for hydrogen production and applications, *Prog. Energy Combust. Sci.*, 2010, 36, 307–326.

[3] C. C. L. McCrory, S. Jung, I. M. Ferrer, S. M. Chatman, J. C. Peters and T. F. Jaramillo, Benchmarking hydrogen evolving reaction and oxygen evolving reaction electrocatalysts for solar water splitting devices, *J. Am. Chem. Soc.*, 2015, 137, 4347–4357.

[4] Z. W. Seh, J. Kibsgaard, C. F. Dickens, I. Chorkendorff, J. K. Norskov and T. F. Jaramillo, Combining theory and experiment in electrocatalysis: insights into materials design, *Science*, 2017, 355, eaad4998.

[5] L. Trotochaud, S. L. Young, J. K. Ranney and S. W. Boettcher, Nickel-iron oxyhydroxide oxygen-evolution electrocatalysts: the role of intentional and incidental iron incorporation, *J. Am. Chem. Soc.*, 2014, 136, 6744–6753.

[6] D. Friebel, M. W. Louie, M. Bajdich, K. E. Sanwald, Y. Cai, A. M. Wise, M.-J. Cheng, D. Sokaras, T.-C. Weng, R. Alonso-Mori, R. C. Davis, J. R. Bargar, J. K. Norskov, A. Nilsson and A. T. Bell, Identification of highly active Fe sites in (Ni,Fe)OOH for electrocatalytic water splitting, *J. Am. Chem. Soc.*, 2015, 137, 1305–1313.

[7] M. S. Burke, M. G. Kast, L. Trotochaud, A. M. Smith and S. W. Boettcher, Cobalt-iron (oxy)hydroxide oxygen evolution electrocatalysts: the role of structure and composition on activity, stability, and mechanism, *J. Am. Chem. Soc.*, 2015, 137, 3638–3648.

[8] P. Liu and J. A. Rodriguez, Catalysts for hydrogen evolution from the [NiFe] hydrogenase to the $Ni_2P(001)$ surface: the importance of ensemble effect, *J. Am. Chem. Soc.*, 2005, 127, 14871–14878.

[9] E. J. Popczun, J. R. McKone, C. G. Read, A. J. Biacchi, A. M. Wiltrout, N. S. Lewis and R. E. Schaak, Nanostructured nickel phosphide as an electrocatalyst for the hydrogen evolution reaction, *J. Am. Chem. Soc.*, 2013, 135, 9267–9270.

[10] X. Zou and Y. Zhang, Noble metal-free hydrogen evolution catalysts for water splitting, *Chem. Soc. Rev.*, 2015, 44, 5148–5180.

[11] T. F. Jaramillo, K. P. Jorgensen, J. Bonde, J. H. Nielsen, S. Horch and I. Chorkendorff, Identification of active edge sites for electrochemical $H_2$ evolution from $MoS_2$ nanocatalysts, *Science*, 2007, 317, 100–102.

[12] D. Merki and X. Hu, Recent developments of molybdenum and tungsten sulfides as hydrogen evolution catalysts, *Energy Environ. Sci.*, 2011, 4, 3878–3888.

[13] C. G. Morales-Guio, L.-A. Stern and X. Hu, Nanostructured hydrotreating catalysts for electrochemical hydrogen evolution, *Chem. Soc. Rev.*, 2014, 43, 6555–6569.

[14] M. S. Faber and S. Jin, Earth-abundant inorganic electrocatalysts and their nanostructures for energy conversion applications, *Energy Environ. Sci.*, 2014, 7, 3519–3542.

[15] S. Anantharaj, S. R. Ede, K. Sakthikumar, K. Karthick, S. Mishra and S. Kundu, Recent trends and perspectives in electrochemical water splitting with an emphasis on sulfide, selenide, and phosphide catalysts of Fe, Co, and Ni: a review, *ACS Catal.*, 2016, 6, 8069–8097.

[16] A. Borah, Pooja, R. Pawar and G. Rajeshkhanna, Synergistically enhanced electronic modulation in trimetallic Cu-Co-Mo-based heterostructured nanomaterials for green $H_2$ production via efficient alkaline electrolysis, *J. Mater. Chem. A*, 2025, 13, 7215–7227.